ISSN 0036-0244, Russian Journal of Physical Chemistry A, 2010, Vol. 84, No. 4, pp. 629–635. © Pleiades Publishing, Ltd., 2010.
Original Russian Text © E.M. Egorova, 2010, published in Zhurnal Fizicheskoi Khimii, 2010, Vol. 84, No. 4, pp. 713–720.

PHYSICAL CHEMISTRY OF NANOCLUSTERS AND NANOMATERIALS

Biochemical Synthesis of Gold and Zinc Nanoparticles in Reverse Micelles

E. M. Egorova

Moscow Research Institute of General Pathology and Pathophysiology, Russian Academy of Medical Sciences, Moscow, 125315 Russia

e-mail: emenano@mail.ru

Received March 23, 2009

Abstract—Gold and zinc nanoparticles were obtained in AOT reverse micelles in isooctane by reduction of the corresponding metal ions by the natural pigment quercetin (the biochemical synthesis technique). Gold and zinc ions were introduced into the micellar solution of quercetin in the form of aqueous solutions, $HAuCl_4$ and $[Zn(NH_3)_4]SO_4$, to the water to AOT molar ratios 1–3 and 3–4, respectively. The process of nanoparticle formation was investigated by spectrophotometry. Nanoparticle size and shape were determined by transmission electron microscopy. The data obtained allow to conclude that there are two steps in metal ion–quercetin interaction: (1) complex formation, and (2) complex dissociation with subsequent formation of nanoparticles and a second product, presumably oxidized quercetin. Gold nanoparticles were found to be of various shapes (spheres, hexahedrons, triangles, and cylinders) and sizes, mainly in the 10–20 nm range; zinc nanoparticles are chiefly spherical and ~5 nm in size. In both cases, the nanoparticles are stable in the air in micellar solution over long periods of time (from a several months to a several years).

DOI: 10.1134/S0036024410040199

INTRODUCTION

The reduction of metal ions in reverse micelles by natural pigments from the group of flavonoids (the method of biochemical synthesis) allows to obtain silver and copper nanoparticles [1–4]. Such nanoparticles have high stability in micellar solution in air, which allows to carry out systematic investigations of their properties and develop various ways for their practical application both in solution and after adding this solution to liquid-phase systems (e.g., coating compositions), or after deposition from solution on various solid surfaces. Ag nanoparticles have been found to possess distinct antimicrobial activity [3, 5–8], whereas Cu nanoparticles are efficient catalysts of the isomerization reaction of dichlorobutenes [3, 9, 10]. High catalytic activity has also been detected for Ag, Cu, Co, and Ni nanoparticles in certain industrial processes of organic synthesis [11]. The feasibility of producing Zn nanoparticles has been demonstrated, the nanoparticles are expected to manifest significantly greater anticorrosion efficiency than the ultradisperse zinc powders currently being produced [12].

In addition to its practical applications, biochemical synthesis in reverse micelles is also interesting in terms of understanding how metal nanoparticles interact with living organisms. This problem has become especially actual in recent years due to the rapid development of applied research involving metal nanoparticles and their application in the production of various commodities (cosmetics, clothes, household appliances, toys, and so on). Investigations of interactions between nanoparticles and living organisms reveal that metal nanoparticles can have a curative effect or cause pathological changes. The possibilities for applying nanoparticles to diagnose and treat various disorders, as well as in immunochemical testing techniques, are already being actively studied and developed in a new area of experimental medicine, *nanomedicine*, and a journal by that name has been published in English since 2004 [13]. Of particular interest in this respect are gold nanoparticles, which have been found useful in enhancing the efficiency of photothermal therapy and radiotherapy in the treatment of oncological diseases [14–16].

At the same time, metal nanoparticles can cause serious illnesses (nanopathologies) in living organisms [17–19]. The problem of elucidating the causes of the pathological effect of metal nanoparticles and developing methods to fight diseases caused by the introduction of these nanoparticles into the human organism is therefore of major interest. The ability to obtain nanoparticles that are stable in solution on the air for prolonged periods of time is obviously essential to the success of such research. It is particularly important to investigate how gold and zinc nanoparticles behave, as they have been found highly bioactive in contact with cells and other biological objects [20–22].

Various techniques for synthesizing gold nanoparticles in aqueous solutions or two-phase systems have been described in the literature as using inorganic or organic reducing agents (including macromolecular

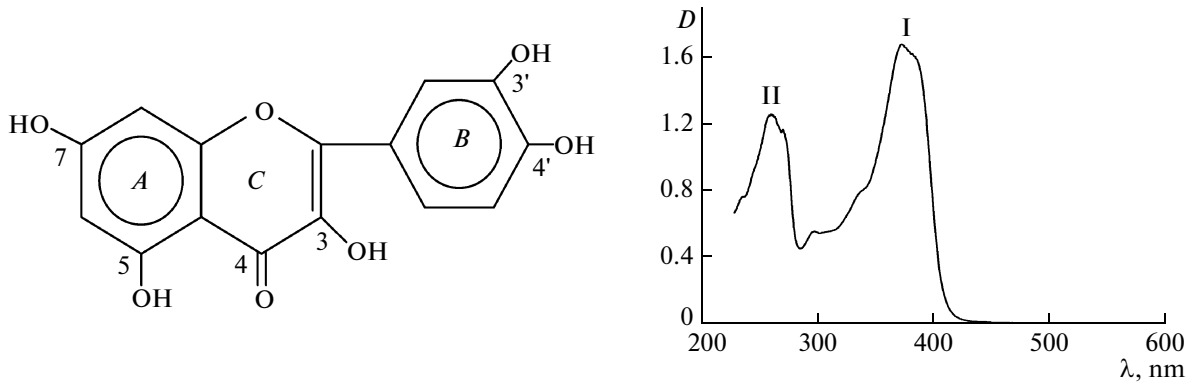

Fig. 1. Structural formula of quercetin and absorption spectrum of quercetin in micellar solution.

agents) [23–27] and reverse micelles with the aid of conventional chemical reducing agents and UV or laser photoreduction [28, 29]. There have also been several reports on the preparation of zinc nanoparticles by laser ablation in water or in aqueous solution of sodium dodecyl sulfate [30], by decomposition of organometallic precursors in a water-organic solvent [31], and by ion implantation into solid matrices [32, 33].

In our work, we report the preparation of air-stable Au and Zn nanoparticles by biochemical synthesis in reverse micelles in the presence of flavonoid quercetin as the reducing agent. We thus propose a combination of reverse micelles whose advantages for the synthesis of metal nanoparticles are sufficiently well-known (e.g., see [28, 34]) and an nontraditional organic reducing agent, quercetin (which, to the best of our knowledge, has never been used either in the preparation of gold sols or in the synthesis of zinc nanoparticles. The work was carried out using spectrophotometric techniques and transmission electron microscopy. Based on the results obtained by analyzing changes in the absorption spectra of micellar solutions, suggestions as to the nanoparticle formation mechanism are offered.

EXPERIMENTAL

In order to produce gold and zinc nanoparticles, aqueous solutions of chloroauric acid ($HAuCl_4 \cdot 3H_2O$, chemically pure) and zinc sulfate ($ZnSO_4 \cdot 7H_2O$, chemically pure) were utilized, respectively. The solutions were prepared with deionized water obtained using a Vodolei set-up (Khimpribor NPO, Russia). A solution of ammonium salt (zinc tetraammonium sulfate) was prepared by adding 10 or 27% aqueous solution of ammonium to an aqueous solution of zinc sulfate until the forming precipitate of metal hydroxide had completely dissolved; the $[Zn(NH_3)_4]^{2+}$ complex cation was formed in the process [35]. In order to produce micellar solutions of quercetin, AOT (sodium bis-(2-dioctyl)sulfosuccinate, Aldrich or Acros), reference isooctane, and quercetine (3,5,7,3',4'-pentahydroxyflavon, Merck) were used.

The standard technique for preparing a micellar solution of quercetin has been described in detail elsewhere [1, 2, 4]. A solution of AOT in isooctane was first prepared, and quercetin (Qr) in powder form was then added and solubilized in it. Quercetin concentration in the micellar solution was determined as described in [2, 4].

For the synthesis of gold nanoparticles, 0.1 M aqueous solution of $HAuCl_4$ was evaporated to half its volume, then diluted with water and added to a micellar solution of quercetin to a concentration of $(3–15) \times 10^{-5}$ M and water content $w = [H_2O]/[AOT] = 1–3$. To obtain zinc nanoparticles, aqueous solution of zinc salt was introduced into a micellar solution of quercetin to a concentration of 3–5 mM and $w = 2.5–4$. AOT concentration in the micellar solution was 0.1–0.15 M for zinc nanoparticles and 0.2–0.35 M for gold nanoparticles. Optical absorbance spectra were recorded either on a Specord M-40 (Carl Zeiss, Germany) or on a Helios-α (Thermo Electronics, GB) spectrophotometer in a 1-mm-thick quartz cuvette at room temperature.

RESULTS AND DISCUSSION

Synthesis of gold nanoparticles

Quercetin in a micellar solution has two main absorption bands (Fig. 1): band I ($\lambda_{max} = 370–372$ nm) and band II ($\lambda_{max} = 256–260$ nm). Band I is due to the chromophore consisting of ring B conjugated with the C_4 carbonyl group; band II, with ring *A* [20, 21]. The weak maximum at 295 nm is presumably due to the presence of a hydroxy group at the C3 atom [1, 36].

Introduction of the aqueous solution of $HAuCl_4$ into the micellar solution of Qr leads to a rapid change in solution color. Bright red coloring first appears and then (within 1–2 min) acquires a violet tint that becomes more intense over the next 10–15 min. Color

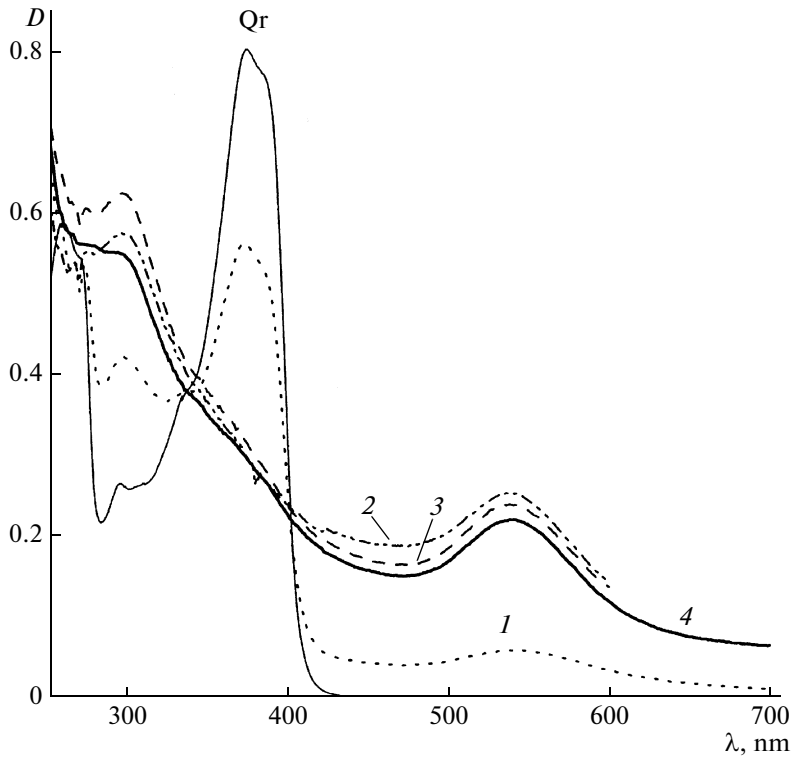

Fig. 2. Formation of gold nanoparticles in micellar solution. Absorption spectra of quercetin (Qr) micellar solution in 2 min (*1*), 15 min (*2*), 1 week (*3*), and 3 months (*4*) after the addition of aqueous solution of $HAuCl_4$; $c(HAuCl_4) = 1.54 \times 10^{-4}$ M, $w = 2$. Initial concentration of quercetin: $c^0_{Qr} = 0.35$ mM.

changes then cease, and the red-violet solution can be preserved over a long time.

Figure 2 shows a typical change in the absorption spectra of a micellar solution of quercetin after the addition of a solution of chloroauric acid (CAA). In the first few minutes, the intensity of band I is reduced as the intensity of the band at 295 nm simultaneously increases, and a weak band in the visible range with a maximum at 535–540 nm appears. Band II remains virtually unchanged. In the following 15–30 min, band I continues to decay and becomes invisible, while the intensities of the two other bands increase. Meanwhile, a clear maximum appears in the visible-range band at 537–538 nm; this band corresponds to the typical range for the absorption maxima of gold nanoparticles (500–550 nm, depending on particle size [25–28]). The life time of this nanoparticle band in our micellar solution varied from a few months to a few years, depending on the parameters of the reverse-micellar system (AOT concentration, *w*, and the Qr/CAA ratio).

The described changes in absorption spectra at the initial stage immediately following the addition of $HAuCl_4$ solution, are similar to those observed during biochemical synthesis of silver nanoparticles at small reagent concentrations [36]. Also observed was a reduction in the intensity of the two main bands of Qr, an intensification of the 295-nm band, and the simultaneous appearance of a band in the absorption region of silver nanoparticles in reverse micelles (420–440 nm). The results from studies of the mechanism of interaction between Qr and silver ions [36] provided the basis for our conclusion that the first stage of interaction is the formation of [Ag^+ ...Qr] complex (by binding of Ag^+ ions with oxygen at the C3 and C4 atoms), reflected on the spectrum by the appearance of the 295-nm band. The complex then undergoes decomposition with the formation of silver atoms and (presumably) oxidized quercetin; the subsequent association of atoms and ions lead to the formation of nanoparticles.

A similar sequence is deemed possible during the synthesis of gold nanoparticles. A complex of quercetin and Au^{3+} ions initially forms (possibly also through oxygen atoms at the C3 and C4 atoms) (Fig. 1). Reduction of gold ions occurs in the complex (possibly via a number of intermediary stages), yielding atoms that subsequently become nuclei for the formation of nanoparticles. Given the recently published calculated enthalpies of formation of quercetin-metal ion complexes [37], the complex might also form via oxygen atoms at the C4 and C5 atoms. Formation of the com-

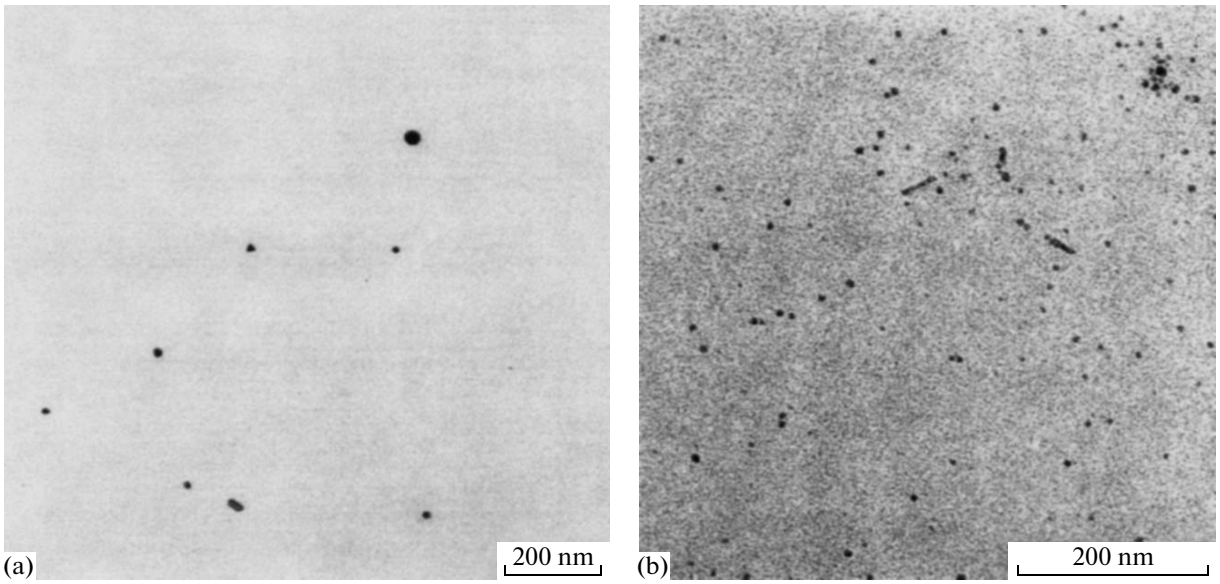

Fig. 3. Electron micrographs of gold (a) and zinc (b) nanoparticles in a micellar solution.

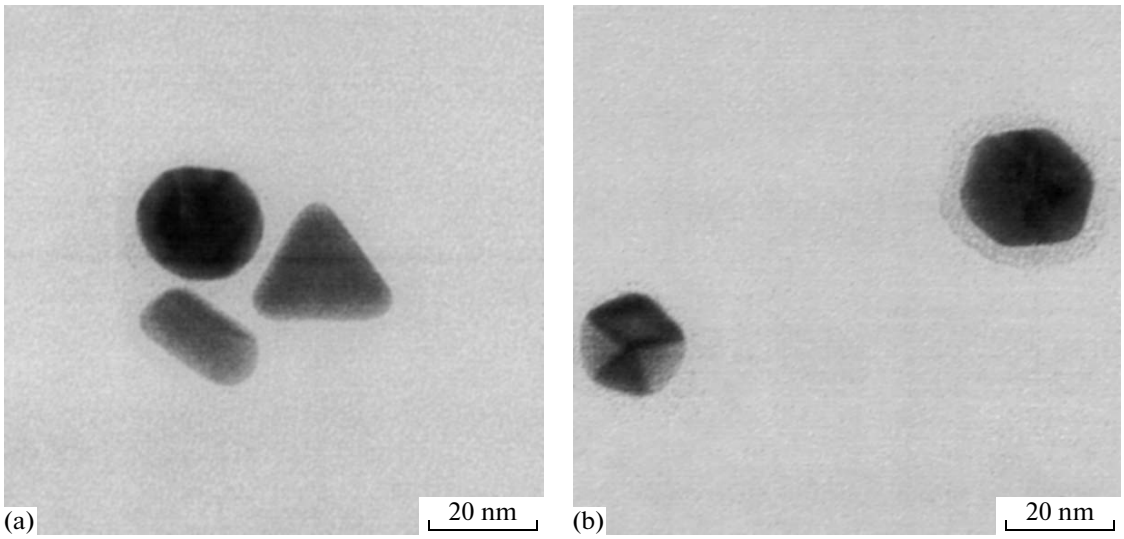

Fig. 4. Micrographs at greater magnification showing various shapes (a) and the crystalline structure (b) of gold nanoparticles.

plex with Au^{3+} ions through oxygen atoms at C4 and C5 in the polyphenol fragment was also suggested by the authors of [27]; they reported the synthesis of gold nanoparticles in aqueous solution using apiin, which is similar to quercetin in structure.

Examples of the electron micrographs of our gold nanoparticle solutions are given in Figs. 3, 4. The nanoparticles have various shapes: hexahedral, pentagonal, triangular, cylindric and spheroidal particles are detectable. The low surface density of the particles in Fig. 3a is due to dilution of the nanoparticle solutions before the preparation of microscopy samples, in order to avoid artifacts caused by high concentrations of the surfactant (AOT) in the micellar solution. As can be seen from the histogram presented in Fig. 5 (for 120 particles), the dimensions of most of the nanoparticles (over 80%) fall within the 10–20 nm range. Histogram processing in the Gaussian approximation yields 16.3 ± 8.5 nm. Photographs at a greater magnification show that the contours of particles are smeared (Fig. 4a); at the same time, many particles have a distinct crystalline structure (Fig. 4b).

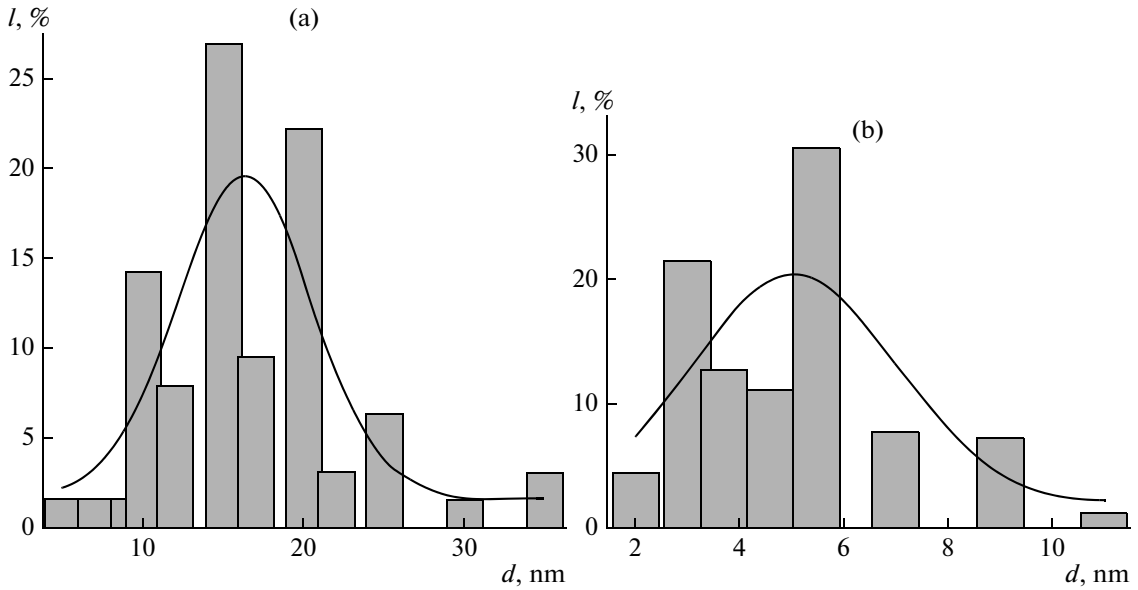

Fig. 5. Particle size distribution histograms in a micellar solution of gold (a) and zinc (b) nanoparticles; *l*, fraction of particles; *d*, diameter.

Synthesis of Zn nanoparticles

In order to produce zinc nanoparticles, we used the logic previously validated in the synthesis of copper nanoparticles [2, 3]. Specifically, the introduction of aqueous solutions of simple copper salts (sulfate, nitrate) into a micellar solution of quercetin was found to yield $[Cu^{2+}...Qr]$ complex. This leads to a bathochromic shift of band I; a similar change in the spectra of flavonoids (including quercetin) is observed during the formation of complexes with copper ions in aqueous solution [38]. There was, however, no subsequent formation of copper nanoparticles. We suggest that the halting of the process at the complex formation stage was due to the two-stage mechanism of the reduction of Me^{2+} ions: first to Me^{+}, then to Me^{0}.

Such distinct stages were observed, for example, during the synthesis of Cu nanoparticles in aqueous solution in the presence of a stabilizing polymer (polyethyleneimine, PEI) that forms a complex with Cu^{+} ions [39]. Since Me^{+} ions are unstable in solution and easily undergo oxidation to the divalent form, the $[Me^{+}...$ Qr] complex does not form and the second stage of reduction therefore does not follow. A similar problem arose during the synthesis of Cu nanoparticles by the radiation–chemical technique in aqueous solution [40, 41]. In order to reduce Cu^{2+} ions to atoms by hydrated electrons, the authors introduced Cl^{-} ions (which form quite stable complexes with Cu^{+} ions) as a stabilizing additive.

Following the same principle, we earlier took advantage of copper ions forming stable complexes with ammonium [35]. We therefore replaced simple copper salts with their complex derivatives by preparing solutions where copper was present in the form of the complex cation $[Cu(NH_3)_4]^{2+}$. Adding these solutions to a micellar solution of Qr, we observed a change in optical absorbance spectra, initially indicating the formation of a cation–quercetin complex and then of Cu nanoparticles [3].

In this work, we also used an ammonium salt (tetraammonium sulfate) obtained by combining aqueous solution of ammonia and zinc sulfate solution for the production of zinc nanoparticles. Addition of aqueous solution containing the $[Zn(NH_3)_4]^{2+}$ complex cation to a micellar solution of Qr leads first to the formation of a complex and then to nanoparticles. Typical changes in absorbance spectra over time are shown in Fig. 6. Complex formation is characterized by a red shift for both bands of quercetin, which is much more noticeable for band I (by 60 nm). As was shown in [38], a similar change in the position of band I in the case of interaction between quercetin and copper ions is caused by the complex formation through OH groups at the C3' and C4' atoms in the *B* ring (Fig. 1). The solution becomes bright-orange. Within a few hours, the complex undergoes rapid decomposition, manifested as a decrease in the intensity of both bands (curves *1–4*). An isosbestic point is also present (373 nm), indicating the formation of a product absorbing at 310–320 nm. Indications as to the nature of this product, as in the case of the formation of Ag and Au nanoparticles, are obtained by investigating the mechanism of antioxidant activity of quercetin, and of its oxidation and interaction with ions of copper and other metals in aqueous solutions (e.g., see [38, 42–44]).

In all cases, the oxidation of quercetin was shown to be accompanied by a shift of an absorption band with a maximum at 320–340 nm, i.e., nearly coinciding

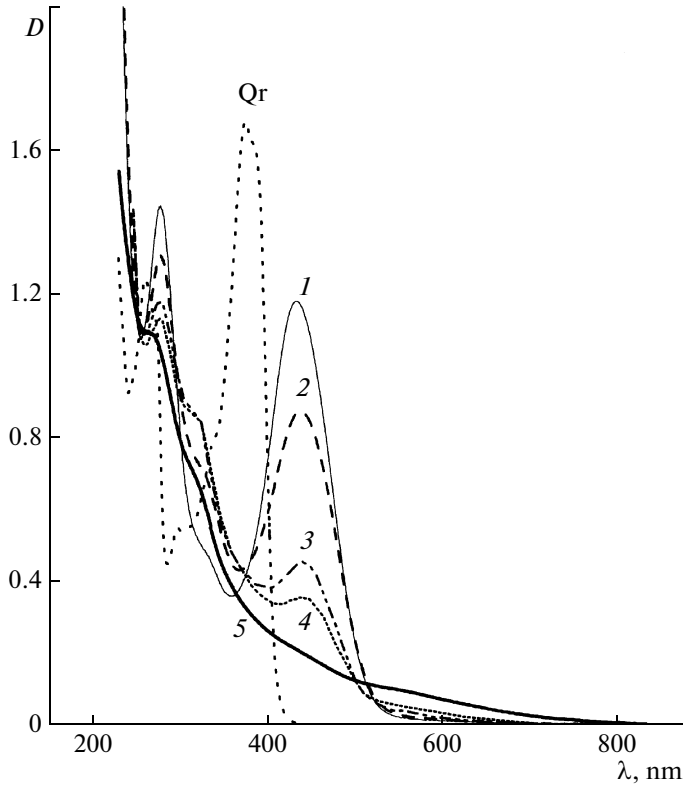

Fig. 6. Formation of Zn nanoparticles in micellar solution. Spectra recorded (*1*) 5, (*2*) 30, (*3*) 70, and (*4*) 100 min and (*5*) 24 h after the addition of aqueous solution of $Zn(NH_3)_4SO_4$; $c^0_{Qr} = 0.59$ mM, $c_{Zn} = 6 \times 10^{-3}$ g-ion/l, $w = 3.7$.

with the band position of the product under question. This allows us to suggest that it belongs to oxidized quercetin.

Slower spectral changes occur over approximately 24 h. The solution turns dark-gray, almost black, which agrees with the solution color changes described in [31] in the case of zinc nanoparticle production by the thermal decomposition of organometallic precursors. Spectral changes then cease; the absorption spectrum of the micellar solution at this stage is shown in Fig. 6 (curve *5*). It is apparent that there are no distinct bands in the solution spectrum, but there are two shoulders in the 250–270 and 310–320 nm regions. For one possible origin of the latter, see the above. As for the 250–270-nm shoulder, it is located in the absorption region of Zn nanoparticles. This follows from the data of [30–33], according to which the absorption band of Zn nanoparticles lies in the 242–285 nm range. Since one of the absorption bands of Qr and its complex with zinc ions lies in the same region, and both these components can remain in the obtained nanoparticle-containing micellar solution (albeit in minor concentrations), it is difficult in our case to isolate the individual band of nanoparticles in the resulting spectrum.

Position of this band can, however, be suggested on the basis of medium polarity dependences of surface plasmon band location of zinc nanoparticles, the dependences being reported in the literature. When these nanoparticles are obtained in aqueous solution, their absorption band lies at 242 nm [30]. A decrease in medium polarity during the synthesis of nanoparticles in silicate glass [32] causes a bathochromic shift of the band to 258 nm. The absorption band of zinc nanoparticles in a sapphire matrix lies in the 260–285 nm range, depending on particle size [33]. Since the medium polarity in reverse micelles at low degrees of hydration is substantially lower than in aqueous solution and can be close to that for the solid matrices, mentioned above, the band in our case can be expected to appear in the 260–285 nm range.

The presence of zinc nanoparticles in the obtained micellar solution was proven by the results of TEM studies. A sample micrograph and particle size distribution histogram are presented in Fig. 5b. It can be seen that the particles are predominantly spherical and small; the diameter of over 80% of the particles is 2–7 nm. The histogram was obtained for 230 particles. Histogram processing in the Gaussian approximation yields a mean size of 5.05 ± 3.94 nm. Also present are rod-shaped particles approximately 5 nm thick and 30–50 nm long.

CONCLUSIONS

In general, the data obtained allow us to conclude that the interaction of CAA and tetraammonium zinc with quercetin in a micellar solution under the conditions of our experiment leads to the formation of gold and zinc nanoparticles that are stable in air over a long period of time. Formation of a quercetin complex of metal ions is the first stage of interaction. In the case of gold, complexes are likely to form via oxygen atoms at the C3 and C4 (the *C* ring) or C4 and C5 (rings *C* and *A*) carbon atoms in the quercetin molecules; in the case of zinc, they form via the OH groups in the *B* ring (Fig. 1). The quercetin complex of metal ions undergoes more or less rapid decomposition with the subsequent formation of metal nanoparticles and a second product, presumably oxidized quercetin.

According to electron microscopy data, gold nanoparticles exist in a variety of shapes, whereas zinc nanoparticles are predominantly uniform (spherical). In addition, a comparison of histograms shows that gold nanoparticles have a greater mean size and vary more in size than zinc nanoparticles. In both cases, however, the nanoparticles are sufficiently small so that we can expect manifestations of their special properties typical of the nanoscale state. In order to study their interaction with biological objects, aqueous solutions of the nanoparticles of both metals were obtained from their micellar solutions using the technique in [45], developed previously for silver nanoparticles. We plan to publish the results from our investi-

gations of the biological effects of gold and zinc nanoparticles in aqueous solutions in future works.

REFERENCES

1. A. A. Revina, E. M. Egorova, and A. D. Karataeva, Zh. Fiz. Khim. **73**, 1897 (1999) [Russ. J. Phys. Chem. A **73**, 1708 (1999)].
2. E. M. Egorova and A. A. Revina, Colloids Surf. A **168**, 87 (2000).
3. E. M. Egorova, A. A. Revina, T. N. Rostovshchikova, and O. I. Kiseleva, Vestn. Mosk. Univ., Ser. Khim. **42**, 332 (2001).
4. E. M. Egorova and A. A. Revina, Kolloidn. Zh. **64**, 334 (2002) [Colloid. J. **64**, 301 (2002)].
5. A. A. Revina, E. M. Egorova, and B. B. Kudryavtsev, Khim. Prom-st., No. 4, 28 (2001).
6. B. B. Kudryavtzev, O. L. Figovsky, E. M. Egorova, et al., J. Sci. Israel-Technol. Advantages, No. 5, 209 (2003).
7. E. M. Egorova, Nanotekhnika, No. 1, 15 (2004).
8. E. M. Egorova, in *Proc. of the Intern. Sci.-Pract. Conf. on Nanotechnologies to Industry 2005, Fryazino, 2005* (Moscow, 2006), p. 26.
9. A. A. Revina, E. M. Egorova, T. N. Rostovshchikova, and O. I. Kiseleva, in *Proc. of the 12th Symp. on Modern Problems of Chemical Physics* (Tuapse, 2000), p. 182.
10. A. A. Revina, E. M. Egorova, T. N. Rostovshikova, et al., Abstr. of the Intern. Conf. Colloids 2000, Szegel, Hyngary, Sept. 2000.
11. A. I. Leont'eva, V. I. Petrik, E. M. Egorova, and T. P. D'yachkova, in *Proc. of the 5th Intern. Sci.-Pract. Conf. on Study, Development and Application of High Technologies in Industry* (Politekhn. Univ., St. Petersburg, 2008), p. 235.
12. T. N. Ostanina, V. M. Rudoi, O. V. Yaroslavtseva, and A. S. Solov'ev, in *Proc. of the 7th Intern. Frumkin Symp.* (Moscow, 2000), p. 530.
13. L. P. Baloh, Nanomed.: Nanotechnol., Biol. Med. **5** (1), 1 (2009).
14. Ivan H. El-Sayed and Mostafa A. El-Sayed, Nanomedicine **2**, 681 (2007).
15. D. Pissuwan, S. M. Valenzuela, and M. B. Cortie, Trends Biotechnol. **24**, 62 (2006).
16. P. Mukherjee, R. Bhattacharya, N. Bone, et al., J. Nanobiotechnology **5** (4) (2007).
17. B. T. Mossman, P. J. Borm, V. Castranova, et al., Part. Fibre Toxicol. **4** (4) (2007).
18. A. Elder, R. Gelein, V. Silva, et al., Environm. Health Perspect. **114**, 1172 (2006).
19. S. Takenaka, E. Karg, C. Roth, et al., Environm. Health Perspect. **109**, 547 (2001).
20. Cha, Kyung Eun, and Myungj Heejoon, Microbiol. Biotechnol. **17**, 1573 (2007).
21. NormanR. Sean, J. W. Stone, A. Gole, et al., Nano Lett. **8**, 302 (2008).
22. J. F. Hillyer and R. M. Albrecht, J. Pharm. Sci. **90**, 1927 (2001).
23. D. A. Handley, *Colloidal Gold. Principles, Methods and Applications*, Ed. by M. A. Hayat (Academic, San Diego, 1989), Vol. 1, Ch. 2.
24. D. V. Leff, P. C. Ohara, J. R. Heath, and W. M. Gelhart, J. Phys. Chem. **99**, 7036 (1995).
25. L. A. Dykman, A. A. Lyakhov, V. A. Bogatyrev, and S. Yu. Shchegolev, Kolloidn. Zh. **60**, 757 (1998) [Colloid. J. **60**, 700 (1998)].
26. M. M. Maye, L. Han, N. N. Kariuki, et al., Anal. Chim. Acta **496**, 17 (2003).
27. J. Kasthuri, S. Veerapandian, and N. Rajendiran, Colloids Surf. B **68**, 53 (2009).
28. J. P. Wilcoxon, R. L. Williamson, and R. Baugham, J. Chem. Phys. **98**, 9933 (1993).
29. V. Arcoleo and Liveri V. Turco, Chem. Phys. Lett. **258**, 223 (1996).
30. H. Zeng, W. Cai, Y. Li, J. Hu, and P. Liu, J. Phys. Chem. B **109**, 18260 (2005).
31. F. Rataboul, C. Nayral, M.-J. Casanove, et al., J. Organomet. Chem. **643–644**, 307 (2002).
32. H. Amekura, N. Umeda, K. Kono, et al., Nanotecnology **18**, 395707 (2007).
33. X. Xiang, X. T. Zu, S. Zhu, et al., Nucl. Instrum. Methods Phys. Res. B **250**, 192 (2006).
34. B. H. Robinson, A. N. Khan-Lodhi, and T. Towey, *Structure and Reactivity in Reverse Micelles*, Ed. by M. P. Pileni (Elsevier, Amsterdam, Oxford, New York, 1989), p. 198.
35. W. Schröter, K.-H. Lautenschläger, H. Bibrack, et al., *Handbook in Chemistry* (Deutsch Harri, 2001; Khimiya, Moscow, 2000).
36. E. M. Egorova and A. A. Revina, Zh. Fiz. Khim., No. 9, 1683 (2003) [Russ. J. Phys. Chem. A **77**, 1513 (1999)].
37. A. D. Roshal' and T. V. Sakhno, Vestn. Khar. Nats. Un-Ta, Khim., No. 532 (7), 123 (2001).
38. J. E. Brown, H. Khoor, R. C. Hider, et al., Biochem. J. **330**, 1173 (1998).
39. T. Sosebee, M. Giersig, A. Holzwarth, et al., Ber. Bunsen-Ges. Phys. Chem. **99** (1), 40 (1995).
40. B. G. Ershov, Usp. Khim. **66** (2), 103 (1997).
41. N. L. Sukhov, M. A. Akinshin, and B. G. Ershov, Khim. Vys. Energ. **20**, 392 (1986).
42. I. B. Afanas'ev, A. I. Dorozhko, A. V. Brodskii, et al., Biochem. Pharmacol. **38**, 1763 (1989).
43. D. Metodieva, A. K. Jaiswal, N. Cenas, et al., Free Radical Biol. Med. **26**, 107 (1999).
44. I. G. Zenkevich, A. Yu. Eshchenko, S. V. Makarova, and V. A. Utsal', Rastit. Resur. **43**, 111 (2007).
45. E. M. Egorova, A. A. Revina, B. V. Rumyantsev, et al., Zh. Prikl. Khim. **75**, 1620 (2002) [Russ. J. Appl. Chem. **75**, 1585 (2002)].